The *Bacillus subtilis* cell envelope stress-inducible *ytpAB* operon modulates membrane properties and contributes to bacitracin resistance

Jessica R. Willdigg[a], Yesha Patel[a], Briana E. Arquilevich[a], Chitra Subramanian[b], Matthew W. Frank[b], Charles O. Rock[b †], John D. Helmann[a]#

[a]Department of Microbiology, Cornell University, Ithaca, NY, USA, 14853-8101

[b]Department of Host Microbe Interactions, St. Jude Children's Research Hospital, Memphis, Tennessee 38105

Running title: ***ytpAB* operon modulates membrane properties**

#Address correspondence to: John D. Helmann, Email: jdh9@cornell.edu

† deceased (9.22.23)

Abstract

Antibiotics that inhibit peptidoglycan synthesis trigger the activation of both specific and general protective responses. σ^M responds to diverse antibiotics that inhibit cell wall synthesis. Here, we demonstrate that cell wall inhibiting drugs, such as bacitracin and cefuroxime, induce the σ^M-dependent *ytpAB* operon. YtpA is a predicted hydrolase previously proposed to generate the putative lysophospholipid antibiotic bacilysocin (lysophosphatidylglycerol), and YtpB is the branchpoint enzyme for the synthesis of membrane-localized C_{35} terpenoids. Using targeted lipidomics we reveal that YtpA is not required for the production of lysophosphatidylglycerol. Nevertheless, *ytpA* was critical for growth in a mutant strain defective for homeoviscous adaptation due to a lack of genes for the synthesis of branched chain fatty acids and the Des phospholipid desaturase. Consistently, overexpression of *ytpA* increased membrane fluidity as monitored by fluorescence anisotropy. The *ytpA* gene contributes to bacitracin resistance in mutants additionally lacking the *bceAB* or *bcrC* genes, which directly mediate bacitracin resistance. These epistatic interactions support a model in which σ^M-dependent induction of the *ytpAB* operon helps cells tolerate bacitracin stress, either by facilitating the flipping of the undecaprenyl-phosphate carrier lipid or by impacting the assembly or function of membrane-associated complexes proteins involved in cell wall homeostasis.

Importance

Peptidoglycan synthesis inhibitors include some of our most important antibiotics. In *Bacillus subtilis*, peptidoglycan synthesis inhibitors induce the σ^M regulon, which is critical for intrinsic antibiotic resistance. The σ^M-dependent *ytpAB* operon encodes a predicted hydrolase (YtpA) and the enzyme that initiates the synthesis of C_{35} terpenoids (YtpB). Our results suggest that YtpA is critical in cells defective in homeoviscous adaptation. Further, we find that YtpA

functions cooperatively with the BceAB and BcrC proteins in conferring intrinsic resistance to bacitracin, a peptide antibiotic that binds tightly to the UPP lipid carrier that sustains peptidoglycan synthesis.

Introduction

The bacterial cell envelope, minimally consisting of a plasma membrane and a peptidoglycan cell wall, is the major barrier between the cell interior and the extracellular environment (1). Peptidoglycan is a rigid and highly cross-linked structure that confers cell shape and resists turgor pressure to prevent lysis. It is also the target of some of the most clinically relevant antibiotics (2). When exposed to changing environmental conditions, including antibiotics, bacteria respond through dedicated cell envelope stress response (CESR) pathways and modulate gene expression to protect the integrity of the cell envelope (3, 4).

Following exposure to a cell envelope stress, an extracellular signal must be communicated across the cell envelope to mediate a transcriptional response. Bacterial CESRs are commonly controlled by two component system (TCS) regulatory networks or by alternative σ factors (often members of the extracytoplasmic function or ECF σ family) which are in turn regulated by stress-responsive anti-σ factors (4-6). For example, the *Bacillus subtilis* BceRS TCS responds selectively to the peptide antibiotic bacitracin that binds to undecaprenyl-pyrophosphate (UPP) and inhibits the recycling of lipid II (7, 8). Activation of the BceRS system upregulates BceAB, an ABC transporter and a primary determinant of intrinsic bacitracin resistance (8). BceAB acts through a target protection mechanism to release bacitracin from inhibited UPP:bacitracin complexes (9). The BceAB complex also collaborates with the BceS sensor kinase to respond to bacitracin stress in a flux-sensing mechanism (10, 11).

In addition to TCSs, ECF σ factors play a prominent role in the regulation of CESRs (4, 6, 12). Upon sensing a cell envelope stress, the membrane-embedded anti-σ factor is inactivated (often by proteolytic cleavage) to release the active σ factor (13-16). One such ECF σ, σ^M, is activated by cell wall targeting antimicrobials (17-20), although the precise σ^M activating stimulus is unclear. The activation of σ^M induces the expression of nearly 100 genes, many of which are involved in peptidoglycan synthesis, cell shape determination, and cell division (6, 18). Consistently, deletion of *sigM* sensitizes the cell to β-lactams (21), moenomycin (20), bacitracin (17), and other antibiotics that target peptidoglycan synthesis (22).

The large σ^M regulon includes several operons with poorly characterized roles in responding to envelope stress (18). The *ytpAB* operon is one such example. Previously, the *ytpA* gene product was assigned as a class A_2-phospholipase that cleaves the *sn2* acyl chain from phosphatidylglycerol (PG) to produce a discrete lysophospholipid (1-(12-methyltetradecanoyl)-3-phosphoglyceroglycerol). This lysophospholipid has been named bacilysocin, and was suggested to function as an antibiotic to inhibit growth of neighboring microorganisms (23). However, purified bacilysocin has weak antibiotic activity with an MIC for *Saccharomyces cerevisiae* of 5 µg/ml and 25 µg/ml for *Staphylococcus aureus* (23), and there is no evidence that it is released into the media at levels sufficient to demonstrate antibiotic activity.

The second gene in the operon, *ytpB*, encodes an enzyme required for sesquarterpenoid synthesis (tetraprenyl-β-curcumene synthase) (24, 25). Sesquarterpenoids are 35 carbon (C_{35}) cyclic compounds derived from heptaprenyl-pyrophosphate (HPP) and have a multi-ring structure similar to C_{30} hopanoids, which are derived from squalene (26). The major sesquarterpenoid made by *B. subtilis* is designated baciterpenol A (24), which can be further modified by autooxidation and dehydration (under non-physiological isolation conditions) to

generate baciterpenol B and sporulenes (27). Deletion of *ytpB* leads to a modest increase in cell sensitivity towards bacitracin (28). Our previous findings revealed that this effect results from increased accumulation of the YtpB substrate, HPP (28). The linear C_{35} HPP isoprenoid is a structural analog of the longer C_{55} isoprenoid, UPP, and both contain a membrane-proximal pyrophosphate moiety, which is the ligand for bacitracin (29).

Here, we have explored the role of YtpA, a putative phospholipase, on membrane properties and bacitracin sensitivity. Overexpression of *ytpA* increased membrane fluidity, but in contrast with a prior report (23), YtpA was not required for lysophosphatidylglycerol (LPG) production. Genetic studies reveal that *ytpA* is critical for the fitness of cells defective in homeoviscous adaptation. Moreover, YtpA contributes to bacitracin resistance in parallel with the BceAB and BcrC resistance systems. We propose that YtpA may support peptidoglycan synthesis by modulating membrane properties to enhance the function of the synthetic machinery and perhaps to facilitate the transmembrane flipping of the UP carrier lipids (30).

Results

Overexpression of YtpA increases membrane fluidity

In previous studies, YtpA was identified as a lysophospholipase responsible for synthesis of bacilysocin (1-(12-methyltetradecanoyl)-3-phosphoglycerol (1-15-LPG)), a lysophospholipid derived from phosphatidylglycerol with a 15 carbon anteiso branched chain fatty acid (23). In eukaryotes, lysophospholipids participate in membrane remodeling via the Lands' cycle in which phospholipids can be deacylated and then reacylated with chemically distinct fatty acids (31). However, the presence of this type of membrane remodeling pathway in bacteria has yet to be established (32). If lysophospholipids persist within the membrane bilayer, they may alter local

membrane curvature, permeability, and fluidity (33-35).

To determine if YtpA impacts membrane fluidity we used the membrane intercalating dye 1,6-diphenyl-1,3,5-hexatriene (DPH) to perform fluorescence anisotropy (FA) (36). The rotational freedom of DPH in the membrane serves as an indicator of membrane fluidity. There was no significant difference in FA between the *B. subtilis* 168 (*trpC2*) wild-type strain (WT) and an isogenic *ytpA* null strain (Δ*ytpA*) (Figure 1). However, since the *ytpAB* operon is known to be stress-inducible (18) this may simply mean that *ytpA* is poorly expressed under these growth conditions. Therefore, we tested the effect of YtpA overexpression using an IPTG-inducible promoter. Indeed, expression of *ytpA* led to a decrease in FA compared to the WT and Δ*ytpA* strain (Figure 1). This suggests an increase in rotational freedom, which is indicative of an increase in membrane fluidity (36). In a previous study, DPH measurements of FA in vesicles made from *B. subtilis* membrane lipids revealed a near linear decrease in FA (an increase in fluidity) over the temperature range from 10 ˚C to 45 ˚C (37). The change observed here between WT cells and those with induction of *ytpA* is comparable to vesicles incubated at temperatures differing by 15-20 ˚C (37). Further, a similar magnitude of change was seen in *B. subtilis* cells with and without induction of the σ^W-dependent membrane stress response, which significantly protects cells against detergents and other agents that increase fluidity (38). Thus, the effect seen here is likely to be physiologically significant.

Induction of *ytpA* rescues growth of cells defective in homeoviscous adaptation

To test if the membrane fluidizing effect noted upon induction of *ytpA* is physiologically relevant, we took advantage of a reporter strain with an artificially rigid membrane (39). This strain, designated Δ*bkd*, is defective in homeoviscous adaptation to conditions of low fluidity due

to deletions of the *bkd* operon and the *des* gene. These mutations prevent the synthesis of branched chain fatty acids (BCFA) and the desaturation of acyl chains by the Des desaturase, respectively (39). Approximately 90% of the *B. subtilis* membrane is composed of BCFAs that help confer an optimal fluidity necessary for the maintenance of the electron transport chain (40). As a result, the Δ*bkd* strain requires supplementation with precursors to BCFAs for normal growth. For example, supplementing with 2-methylbutyric acid (MB) restores the ability to synthesize *anteiso* BCFAs and rescues growth in minimal medium (39).

The Δ*bkd* strain has a minor growth defect compared to WT when grown on LB medium at 27 °C, 37 °C and 45 °C. However, on deletion of *ytpA* (Δ*bkd* Δ*ytpA*), fitness was dramatically reduced. The colony size of the Δ*bkd* Δ*ytpA* strain was very small compared to both the WT and Δ*bkd* strain under all the temperatures tested (Figure 2A). As previously reported, the Δ*bkd* strain is inviable at 22 °C on minimal medium lacking BCFA precursors (Figure 2B). Remarkably, Δ*bkd* with a copy of *ytpA* expressed from the *spac(Hy)* promoter is able to grow at 22 °C, and if MB is additionally present this strain grows as well as WT (Figure 2B). The rescue of growth by YtpA is observed both with and without addition of the inducer IPTG, consistent with the known leaky expression of the *spac(Hy)* promoter (41). Using real time PCR we estimate that the leaky expression from this promoter leads to a two-fold increase in gene expression compared to its native expression in the WT cells. These results suggest that *ytpA* expression is critical to compensate for the growth-limiting defects that define the Δ*bkd* strain.

We next used FA to test if induction of YtpA increases membrane fluidity of the Δ*bkd* strain (Figure 2C). As reported previously (39), the Δ*bkd* strain shows an increase in FA compared to WT. Induction of *ytpA* in the Δ*bkd* strain led to a significant decrease in FA, although not a complete restoration back to the levels of WT cells (Figure 2C). This is consistent

with the partial rescue of growth by induction of *ytpA* in the Δ*bkd* strain at 22 °C in the absence of MB (Figure 2B). We conclude that expression of YtpA increases membrane fluidity and restores growth of a strain defective in biochemical pathways that normally serve to increase membrane fluidity.

YtpA is not the major phospholipase *in vivo*

YtpA was proposed to be a phospholipase A_2 responsible for the release of 1-(12-methyltetradecanoyl)-3-phosphoglycerol (1-15-LPG) into the medium (23). Because lysophospholipids may impact membrane biology, we performed a targeted lipidomic analysis to determine if deletion of *ytpA* altered the phospholipid and lysophospholipid content of the cell. In both the WT and *ytpA* mutant strain (Δ*ytpA*), the major phosphatidylglycerol (PG) and phosphatidylethanolamine (PE) species were the same, with the most abundant species having a total of 30, 31, or 32 carbons in the acyl chains, with a C_{15} fatty acid in the 2-position. The minor 28-PG/PE and the 29-PG/PE peaks have a C_{13} or C_{14} acyl chain in the 2-position, respectively (Supplementary Figure 1A and 1B).

Next, we analyzed the lysophosphatidyglycerol (LPG) and lysophosphatidylethanolamine (LPE) composition of cells (Figure 3 and Supplementary Figure 1C, 1D, 2). For quantitation, the signals arising from the 1- and 2-acyl-lysophospholipids with the same carbon number were combined. Note that bacilysocin, the previously described C_{15} 1-acyl-lysophospholipid (23), most likely results from the action of an unidentified A_1 phospholipase (producing a 2-acyl-lysophospholipid as the product) followed by fatty acyl chain migration (Supplementary Figure 1), which reaches ~90% at the 1-position at equilibrium (42-44). Similar acyl chain migration was seen in recent studies monitoring lysophospholipid production in *Staphylococcus aureus*

(45).

In growing cells and in the medium, the dominant lysophospholipid was 15-LPG (Figure 3A, 3B), with minor amounts of 13- and 14-LPG in cells (Figure 3A). 15-LPE was also a major species in both cells (Figure 3C) and media (Figure 3D) in late-log phase. There was a modest, but statistically significant, reduction in lysophospholipids in the Δ*ytpA* strain in growing cells (Figure 3A, 3C). There was little if any effect noted in stationary phase cells (Supplementary Figure 2A, 2C). One notable change in the stationary phase cultures was that the amount of lysophospholipids in the medium was significantly elevated (10-fold) compared to samples taken in late-log phase (Supplementary Figure 2B, 2D). The presence of lysophospholipids in the cellular fraction of the Δ*ytpA* strain suggests that YtpA is not responsible for the bulk of lysophospholipid synthesis in *B. subtilis.* Consistently, induction of *ytpA* with IPTG did not result in an increase in lysophospholipids compared to either the uninduced condition or WT (Supplementary Figure 3).

YtpA is a member of a large superfamily of serine-dependent hydrolases (alpha-beta hydrolases) with a wide variety of substrates. Bioinformatic searches indicate that YtpA is likely a cytosolic-facing, membrane-associated protein. Sequence homology searches consistently yield sequence and domain similarities between YtpA and other phospholipases, including PldB, a poorly characterized phospholipase and the namesake of the COG2267 superfamily. Because traditional homology searches are limited to sequence similarity, we additionally used the YtpA AlphaFold2-generated structure to search protein structure databases using FoldSeek (46-48). Amongst the many proteins with similar predicted structures, biochemical information is available for only a handful. For example, YtpA has 30% identity to a secreted monoacylglycerol hydrolase from *Mycobacterium tuberculosis* (UNIPROT 007427) that hydrolyses glycerol

monoesters of long-chain fatty acids (49, 50). The lack of a clear functional role for YtpA highlights a recurring problem for this large family of alpha/beta hydrolases, enzymes that often still have enigmatic functions (51).

Cell envelope active antibiotics induce expression of *ytpAB* in a σ^M-dependent manner

Next, we evaluated the regulation of *ytpA* in conditions that lead to cell envelope stress. The *ytpAB* operon is regulated by σ^M, an alternative ECF sigma factor that is activated in response to various peptidoglycan synthesis inhibitors and other cell wall stressors (6). Early genome-wide transcriptome studies have revealed that *ytpAB* is most strongly induced by inhibitors of the membrane-associated steps of peptidoglycan biosynthesis, and in particular by those compounds that interfere with the lipid II cycle such as bacitracin and vancomycin (18, 52). This pattern of response is consistent with a recent comprehensive profiling study using both RNA-seq and tiling array methodologies in which bacitracin and vancomycin were the strongest inducers, followed by tunicamycin, moenomycin, and lysozyme (53).

We constructed a luciferase transcriptional reporter to monitor the expression of the *ytpAB* operon in response to cell envelope stresses. Consistent with expectation, the *ytpAB* reporter fusion was strongly induced by high levels of bacitracin (31.25 μg/ml), and this induction was lost if either the σ^M promoter site or the *sigM* gene was deleted (Figure 4). The reporter fusion was also induced by cefuroxime (0.16 μg/ml), a drug that inhibits the activity of enzymes involved in peptidoglycan synthesis. Using real-time PCR, we observed a four-fold induction of *ytpA* after 15 min of treatment with 31.25 μg/ml of bacitracin, and a two-fold increase when cells were grown to mid-log phase in the presence of the same concentration of bacitracin.

Deletion of bacitracin resistance genes (*bcrC, bceAB*) significantly sensitizes the cell to bacitracin and is known to alter the expression of bacitracin-responsive genes (7). While a WT cell had a bacitracin MIC of 125 µg/ml, deletion of the intrinsic bacitracin resistance determinants *bceAB* or *bcrC* significantly reduced the MIC. In a *bceAB* or *bcrC* deletion background, *ytpAB* expression was induced by concentrations of bacitracin as low as 1.25 µg/ml, (Supplementary Figure 4). The observation that *ytpA* expression is induced in response to cell wall acting drugs is suggestive of a role in intrinsic drug resistance.

The *ytpAB* operon confers bacitracin resistance

Next, we sought to determine if the *ytpAB* operon contributes to bacitracin resistance. The individual deletions of *ytpA* (Δ*ytpA*) or *ytpB* (Δ*ytpB*) did not have a significant effect on the growth of the cells with 62.5 µg/ml bacitracin (0.5x MIC). However, the *ytpAB* double mutant (Δ*ytpAB*) had a notable growth lag (Figure 5). An effect of YtpB on bacitracin resistance was noted previously in studies in Mueller-Hinton medium, and was ascribed to the accumulation of the YtpB substrate heptaprenyl-pyrophosphate (HPP), a close chemical analog of UPP (28). HPP likely complexes with bacitracin and may reduce the efficiency of BceAB-dependent detoxification by competition for the active site of the BceAB resistance protein (9). HPP might also serve as a competitive substrate for the BcrC-dependent phosphatase (28). Although Δ*ytpB* did not affect bacitracin resistance under the conditions we tested (LB medium), *ytpA* or *ytpB* together clearly contribute to bacitracin resistance.

Loss of YtpA increases bacitracin sensitivity in strains lacking BcrC or BceAB

We reasoned that if YtpA were contributing to bacitracin resistance by increasing

membrane fluidity, one mechanism might be through facilitation of UP (or UPP) flipping across the membrane. To explore this, we monitored the bacitracin sensitivity of strains defective in recycling of the undecaprenyl carrier lipid due to lack of a UPP phosphatase (BcrC or UppP). The BcrC and UppP phosphatases are individually dispensable, but the double mutant is not viable (54, 55). In the presence of low levels of bacitracin (5 μg/ml) neither the Δ*bcrC* nor the Δ*ytpA* mutants displayed much of a growth lag. However, the Δ*ytpA* Δ*bcrC* double mutant was greatly inhibited with a >4 hr growth lag (Figure 6A). In contrast, there is very little additivity between Δ*ytpA* and Δ*uppP*, even with high bacitracin levels (62.5 μg/ml) (Figure 6B).

Next, we explored the role of YtpA in strains lacking the BceAB resistance pathway. The BceAB proteins function in the dissociation of UPP:bacitracin complexes in a target protection mechanism of resistance (9). Consistent with prior work (9), Δ*bceAB* was highly sensitive to bacitracin with decreased growth observed at 5 μg/ml. At this concentration, the Δ*ytpA* strain was unaffected, wherease the Δ*ytpA* Δ*bceAB* double mutant was unable to grow (Figure 6C). The additivity of YtpA with both BcrC and BceAB, the two major players of bacitracin resistance network, suggest a role for YtpA in bacitracin resistance. By increasing membrane fluidity, YtpA may reduce UPP levels on the outer leaflet of the membrane, perhaps by allowing it to flip inside.

Loss of YtpA has only a small effect in strains lacking the UptA UP flippase

Following the transglycosylation reaction, the UPP lipid carrier is dephosphorylated on the outer leaflet of the membrane. Then, the transmembrane flipping of the UP product is facilitated by DedA family membrane proteins (22, 56). In *B. subtilis*, the σ^M-regulated *uptA* (formerly *yngC* gene) encodes one such protein (22). A null mutant of *uptA* (Δ*uptA*) has no overt

271 growth defect but displays an increased sensitivity to MX-2401 (22), an antibiotic that binds
272 selectively to UP exposed on the outer leaflet of the membrane (57).
273 We speculated that YtpA-dependent membrane changes might also help to support the
274 flipping of UP. However, deletion of *ytpA* did not increase the sensitivity of the *uptA* strain
275 (Δ*ytpA* Δ*uptA*) to the sub-MIC level of 0.6 μg/ml MX-2401 (Figure 7A). Consistent with the
276 notion that UptA mediates flipping of UP but not UPP, the *uptA* deletion (Δ*uptA*) had little effect
277 on bacitracin sensitivity (Figure 7B), as shown previously (22). Moreover, the *ytpA* and *uptA*
278 mutations did not exhibit an additive effect on bacitracin sensitivity (Figure 7B). The absence of
279 additivity with UptA on sensitivity to MX-2401 suggests that YtpA has no significant role in
280 modulating UP levels on the outside of the membrane.
281
282 **Discussion**
283 Antibiotics that interfere with peptidoglycan synthesis activate a large regulon of genes
284 associated with σ^M-dependent promoters that collectively function to sustain cell wall synthesis
285 even if one or more steps are inhibited (6, 18). The σ^M stress response is triggered when the
286 membrane-localized anti-σ^M complex (YhdK/YhdL) is inactivated by a still unknown
287 mechanism (13). Induction is amplified by a very strong positive autoregulation that leads to
288 high level but transient expression from an autoregulatory promoter for the *sigM-yhdL-yhdK*
289 operon (58). Prolonged and un-regulated induction of the σ^M regulon is lethal due, in part, to
290 toxicity from high level production of numerous integral membrane proteins (59). The transient
291 induction of the σ^M stress response can counteract the action of many cell wall-acting antibiotics,
292 and *sigM* mutants display heightened sensitivity to moenomycin, bacitracin, β -lactams, and
293 other peptidoglycan synthesis inhibitors (20, 21).

294 To define the roles of σ^M-activated operons in protection against cell envelope stress we
295 and others have sought to identify σ^M target genes and their functions. This task is complex due
296 to the large number of σ^M-activated operons (18) and the overlapping regulation with other ECF
297 σ-dependent regulons (19-21, 60). In addition, many stress-induced operons, including those for
298 essential genes, are expressed independent of σ^M and then further upregulated in times of stress.
299 The role of σ^M in protecting against peptidoglycan synthesis inhibitors can be attributed,
300 at least in part, to the upregulation of genes for peptidoglycan synthesis. The σ^M regulon includes
301 genes for both cytosolic steps of peptidoglycan biosynthesis (Ddl, MurB, MurF) and membrane-
302 associated steps, including the alternate lipid II flippase (Amj), components of the Rod complex
303 for peptidoglycan assembly (RodA, MreBCD), and a class A PBP (PBP1) (18, 61-63). In the
304 specific case of moenomycin, σ^M regulation of the RodA transglycosylase is sufficient for
305 resistance (61, 63). Other σ^M-activated functions include enzymes for UPP synthesis (IspD, IspF)
306 (64), the BcrC UPP-phosphatase (18, 60, 65), and the UptA UPP flippase (22), which can all
307 function to help sustain sufficient levels of the undecaprenyl-phosphate lipid carrier (7, 64). In
308 addition, σ^M increases synthesis of stress-induced isozymes for synthesis of lipoteichoic acid
309 (LtaSa; (66)) and wall teichoic acid (TagT;(67)). Finally, σ^M activates genes that control
310 secondary stress responses. The latter include genes encoding the SasA(YwaC) small alarmone
311 synthase responsible for generation of (p)ppGpp, pGpp, ppApp, and AppppA (68), the DisA
312 synthase for cyclic-di-AMP, and Spx, a transcription factor that controls a large regulon that
313 contributes to protection from oxidative stress (69).
314 Although the roles of many σ^M-regulated operons have now been defined, there are still
315 others with poorly understood functions. Here, we demonstrate that the *ytpAB* operon contributes
316 to the high level of intrinsic bacitracin resistance characteristic of *B. subtilis*. Bacitracin is a

317 cyclic dodecapeptide metalloantibiotic produced by some *B. licheniformis* and *B. subtilis* species
318 (70). Bacitracin binds together with a Zn^{2+} ion to sequester the pyrophosphate moiety and first
319 prenyl group of the UPP carrier lipid released on the outer leaflet of the membrane following the
320 transglycosylation reaction (29). To sustain the lipid II cycle the UPP carrier must be
321 dephosphorylated to the undecaprenyl phosphate (UP), which is required by the MraY enzyme
322 for the synthesis of lipid I.

323 Consistent with its close genetic relationship to known producer species, *B. subtilis*
324 expresses a robust intrinsic resistance to bacitracin (7, 64). The first line of defense is the BceAB
325 ABC transporter, which dissociates the bacitracin:UPP complex in a target protection mechanism
326 (9). The BceAB transporter is specifically induced by bacitracin through the action of the BceRS
327 two-component system (10). The BceS sensor kinase forms a complex with the BceAB proteins
328 to allow for a flux-sensing regulation mechanism (10, 11). The second line of defense is BcrC, a
329 σ^M-dependent UPP phosphatase (7). By dephosphorylating UPP to UP, BcrC converts the
330 bacitracin target to a form no longer recognized by this antibiotic (65). However, UP is the target
331 for amphomycin antibiotics, including the semi-synthetic derivative MX-2401 (57). Here, we
332 identify the *ytpAB* operon as an additional contributor to intrinsic resistance to bacitracin.

333 YtpA is annotated as a phospholipase responsible for removal of a fatty acyl chain from
334 phosphatidylglycerol to generate a lysophospholid species (bacilysocin) reported to have weak
335 antibiotic activity (23). We have confirmed that *B. subtilis* does produce lysophospholipids,
336 including LPG, detectable both in the supernatant and membrane fractions. However, YtpA is
337 not required for LPG production (Figure 3), nor are lysophospholipid levels enhanced in a strain
338 in which *ytpA* is induced (Supplementary Figure 3). The enzyme, presumably an A_1
339 phospholipase, that is responsible for forming these species remains to be determined, and the

product(s) that result from YtpA activity are also still unclear.

The *ytpAB* operon additionally encodes YtpB, an enzyme that converts heptaprenyl pyrophosphate (HPP) into the monocyclic tetraprenyl-β-curcumene in the committed step in the synthesis of the C_{35} terpenoid designated baciterpenol A (24, 25). Baciterpenol A presumably modulates membrane properties and may thereby contribute to stress resistance, but its physiological role remains poorly characterized. A *ytpB* mutant strain was previously reported to be sensitized to bacitracin, an effect was attributed to an increased accumulation of the substrate, HPP, rather than the absence of product (28). The co-regulation of YtpA and YtpB is consistent with a model in which they both function to modulate membrane properties in response to stress.

We here present evidence that *ytpA* affects membrane fluidity and interacts genetically with proteins that function in homeoviscous adaptation. Specifically, we observed a striking growth defect in Δ*bkd* Δ*ytpA* cells lacking the ability make BCFAs and desaturated phospholipids and also missing YtpA (Figure 2). This indicates that YtpA modulates membrane properties. Whether these effects are due to the modest impact that YtpA has on lysophospholipid synthesis (Figure 3), or by some other mechanism, is still unknown.

YtpA also contributes to intrinsic bacitracin resistance as revealed in cells defective in other intrinsic resistance mechanisms (Figure 6). The known mechanisms of bacitracin resistance all affect the availability of the bacitracin target UPP (BcrC) or the stability of its complex with bacitracin (BceAB) (Figure 8). In *B. subtilis*, there are two UPP phosphatases, UppP and BcrC, and at least one is required for viability (54, 55). Circumstantial evidence suggests that BcrC may be the major UPP phosphatase active on the outer leaflet of the membrane. Specifically, loss of BcrC leads to a significant increase in sensitivity to bacitracin, whereas there is no effect seen with a strain lacking *uppP*, the second UPP phosphatase. The strong additive effect on bacitracin

363 sensitivity between *bcrC* (which increases UPP levels in the outer leaflet) and *ytpA* (Figure 6)
364 suggests that increased membrane fluidity may facilitate UPP flipping, possibly through a
365 spontaneous reaction or one involving an unidentified protein partner (Figure 8). In addition,
366 YtpA may alter membrane properties that affect the function of membrane-anchored enzymes
367 involved in cell wall synthesis.
368
369 **Materials and Methods**
370 **Growth conditions, bacterial strains, and plasmids**
371 All strains were cultured in lysogeny broth (LB) medium at 37 °C and aerated on an
372 orbital shaker at 300 RPM. Before each experiment, glycerol stocks were streaked onto fresh LB
373 agar plates and grown overnight at 37 °C. Antibiotics were used as required at the following
374 concentrations: 100 µg/ml ampicillin; 10 µg/ml chloramphenicol; MLS (1 µg/ml erythromycin
375 and 2.5 µg/ml lincomycin); 10 µg/ml kanamycin. Bacterial strains used in this study are listed in
376 Table 1. Bacitracin was used as the biologically active Zn-salt (Zn bacitracin; Sigma #B5150),
377 unless otherwise indicated. Deletion strains were created utilizing the BKK/BKE genomic library
378 available at the Bacillus Genome Stock Center (BGSC) (71). Taking advantage of the natural
379 competence of *B. subtilis*, all gene deletions with either a kanamycin or an erythromycin cassette
380 were moved into the WT *B. subtilis* 168 strain. For transformation, *B. subtilis* was grown in
381 modified competence media (MC) to stationary phase ~0.8-1.0 OD_{600nm}, incubated with desired
382 DNA for 1-2 hours, and plated on appropriate antibiotics. Null mutations were created by
383 removing the antibiotic resistance cassette to create clean, in-frame deletion mutants using the
384 pDR244 plasmid, as described (71). All gene deletions were confirmed via colony PCR using
385 designated check primers (Table S1). Genes were overexpressed ectopically at the *amyE* locus

386 using the pPL82 plasmid (72). Ectopic overexpression from the *Pspac(hy)* promoter was induced
387 with 1 mM IPTG. Long-flanking homology PCR was used to construct operon deletions using
388 primers as shown in Table S1. The *Δbkd* strain contains a deletion of the entire *bkd* operon (*ptb,*
389 *bcd, ipdV, bkdAA, bkdAB,* and *bkdB*), in addition to a *des* deletion (39).
390
391 **Fluorescence Anisotropy**
392 Fluorescence anisotropy was performed as described with modification (73). Briefly, 5
393 ml of cells were grown in LB medium at 37 °C with shaking to an OD_{600nm} ~1.0 with or without
394 1 mM IPTG induction, where applicable. Cells were harvested and centrifuged at 2500 x g for 3
395 minutes. Cell pellets were washed twice and then resuspended in phosphate buffer (100 mM, pH
396 7.0) to OD_{600nm} 0.15. Cells were treated with 1,6-diphenyl-1,3,5-hexatriene (DPH) (Sigma) to a
397 final concentration of 3.2 µM. An unlabeled control was also prepared. Cells were incubated in
398 the dark in a 30 °C water bath for 30 minutes. Fluorescence anisotropy was performed with a
399 PerkinElmer LS55 luminescence spectrometer (λ_{ex} = 358 nm, slit width = 10 nm; λ_{em} = 428 nm,
400 slit width = 15 nm). A correction for the fluorescence intensity of unlabeled cells was performed
401 as described (74). Data averages and standard deviations of 3 biological replicates are shown.
402
403 **Spot dilution assay**
404 Cells were streaked onto LB agar plates and grown overnight at 37 °C. From a colony, 5
405 mL cells were grown in LB till ~ 0.4 OD_{600nm}. Ten-fold serial dilutions were prepared and 5 uL
406 of the cells were plated on LB medium. Plates were allowed to air dry for 20 minutes and then
407 incubated at 27, 37, and 42 °C. Images were captured after two days for plates incubated at 27 °C
408 and 1 day for plates incubated at 37 and 42 °C. For the cold sensitivity assay, cells were streaked

onto LB agar plates supplemented with 100 µM 2-methylbutyric acid (MB) (Sigma), and grown at 37 °C. 5 ml of cells were grown from an isolated colony in LB medium in the absence of 2-methylbutyric acid at 37 °C to ~1.0 OD_{600nm}. Cells were harvested and centrifuged at 2500 x g for 5 minutes, and the pellets were washed with an equal volume of standard lab minimal media (15 mM $(NH_4)_2SO_4$, 0.8 mM $MgSO_4$ $7H_2O$, 3.4 mM sodium citrate dihydrate, 2 mM KPO_4, 4.2 mM potassium glutamate, 40 mM morpholinepropanesulfonic acid (MOPS), pH 7.4, 0.25 mM tryptophan, 5 µM $FeSO_4$, 5 µM $MnCl_2$, 2 % glucose). Ten-fold serial dilutions were performed in minimal medium, and 10 µL of cells were spotted onto minimal medium plates. Plates were allowed to air dry for 20 minutes and then incubated at 22 °C temperatures. Minimal media agar plates were either unsupplemented, supplemented with 100 µM MB, or supplemented with 1 mM IPTG. Spot dilutions were photographed every 24 hours to monitor growth. N = 3. A representative image is shown.

LPG/LPE mass spectrometry

WT and *ytpA* deletion strains were grown in LB media till late-log phase and over-night for stationary phase cultures. For the strains harboring IPTG-inducible *ytpA*, cells were grown with or without 1 mM IPTG till late-log phase. LPG/LPE were extracted from 5 mL of cells or 1 mL of supernatant from 0.2 µm filtered media. The cells were resuspended in 0.5 mL water and 0.5 mL of cold methanol containing 1% acetic acid was added. To the 1 mL of filtered media, 1 mL of cold methanol containing 1% acetic acid was added. Samples were incubated on ice for 10 min and centrifuged at 20,000 × g for 20 min. Supernatants were dried in a speed vac concentrator and resuspended in 80% methanol containing 100 ng/mL of [d5]17-LPG.

LPG and LPE were analyzed using a Shimadzu Prominence UFLC attached to a QTrap

4500 equipped with a Turbo V ion source (Sciex). Samples were injected onto an Acquity UPLC HSS C18, 2.5mm, 3.0 x 150 mm column at 30°C (Waters) using a flow rate of 0.2 mL/min. Solvent A was 5 mM ammonium acetate + 1% formic acid, and Solvent B was 95% methanol + 5 mM ammonium acetate + 1% formic acid. The HPLC program was the following: starting solvent mixture of 35% A/65% B, 0 to 1 min isocratic with 65% B; 1 to 3 min linear gradient to 100% B; 3 to 30 min isocratic with 100% B; 30 to 32 min linear gradient to 65% B; 32 to 35 min isocratic with 65% B. The QTrap 4500 was operated in the negative mode, and the ion source parameters were: ion spray voltage, -4500 V; curtain gas, 30 psi; temperature, 500°C; collision gas, medium; ion source gas 1, 20 psi; ion source gas 2, 35 psi; declustering potential, -80 V; and collision energy, -30 V. The multiple reaction monitoring (MRM) transitions for LPG and LPE species are listed in Table S2. [d5]17-LPG was used as the internal standard. The system was controlled by the Analyst software (Sciex) and analyzed with MultiQuant 3.0.2 software (Sciex). Peaks corresponding to individual LPG species were quantified relative to the internal standard.

Phosphatidylglycerol (PG) mass spectrometry

WT and *ytpA* deletion strains were grown in LB media till late-log phase. Lipids were extracted from 5 mL of culture by the Bligh and Dyer method. Lipid extracts were resuspended in chloroform/methanol (1:1). PG was analyzed using a Shimadzu Prominence UFLC system attached to a QTrap 4500 equipped with a Turbo V ion source (Sciex). Samples were injected onto an Acquity UPLC BEH HILIC, 1.7 µm, 2.1 × 150 mm column (Waters) at 45 °C with a flow rate of 0.2 mL/min. Solvent A was acetonitrile, and solvent B was 15 mM ammonium formate, pH 3. The HPLC program was the following: starting solvent mixture of 96% A/4% B; 0 to 2 min, isocratic with 4% B; 2 to 20 min, linear gradient to 80% B; 20 to 23 min, isocratic

455 with 80% B; 23 to 25 min, linear gradient to 4% B; 25 to 30 min, and isocratic with 4% B. The
456 QTrap 4500 was operated in the Q1 negative mode. The ion source parameters for Q1 were as
457 follows: ion spray voltage, −4500 V; curtain gas, 25 psi; temperature, 350 °C; ion source gas 1,
458 40 psi; ion source gas 2, 60 psi; and declustering potential, −40 V. The system was controlled
459 and analyzed by the Analyst software (Sciex).
460 The samples were introduced to the QTrap 4500 by direct injection to perform product
461 scans to verify the fatty acids present in a particular PG molecular species along with the
462 positional distribution of the fatty acids. The ion source parameters for negative mode product
463 scan were as follows: ion spray voltage, −4500 V; curtain gas, 10 psi; collision gas, medium;
464 temperature, 270 °C; ion source gas 1, 10 psi; ion source gas 2, 15 psi; declustering potential,
465 −40 V; and collision energy, −50 V.
466
467 **Luciferase reporter construction and measurement**
468 Luciferase reporters were constructed by inserting designated promoters into the multiple
469 cloning site of pBS3E*lux*, or pBS3K*lux* (75) and transformed into *B. subtilis* using natural
470 competence as described above. For luciferase measurements, strains were grown in LB medium
471 at 37 °C to ~0.4 OD_{600nm}. 2 µl of culture was inoculated into 99 µl of fresh LB medium in a 96
472 well plate. Where applicable, cultures were treated with 0.005 µg/ml cefuroxime. The
473 concentration of bacitracin used varied depending on the strains and has been mentioned in the
474 figure legend. The plate was incubated at 37 °C with orbital shaking in a Synergy H1 plate reader
475 (BioTek Instruments, Inc,) and OD_{600nm} and luminescence was measured every 6 minutes.
476 Relative light units (RLU) for promoter activity were determined by luciferase intensity
477 normalized for cell density (OD_{600nm}). Data shown is the representative average and standard

478 deviations of 3 biological replicates.

479

480 **Growth kinetics assay**

481 From a single colony, cells were grown in 5 ml LB medium at 37 °C with shaking to
482 OD_{600nm} ~ 0.4-0.5. 1 µL of culture was added to 199 µL of fresh LB medium in a 100-well
483 Honeycomb plates (Steri). Where applicable, cells were treated with sub-lethal concentrations of
484 bacitracin as determined by the relative bacitracin sensitivity of each strain. The OD_{600nm} of each
485 well was measured at 37°C with shaking in a Bioscreen C Pro growth analyzer (Growth Curves
486 USA, NJ) every 30 minutes for 24 hours. Data shown are representative plots and standard
487 deviations are from three biological replicates.

488

489 **Real-time PCR**

490 Gene expression was determined by real-time PCR using primers mentioned in Table S1.
491 Cultures were grown up to an OD_{600nm} of ~0.4. RNA was purified from 1.5 mL of cells using the
492 RNeasy kit from Qiagen as per the manufacturer's instructions. The isolated RNA was then
493 given a DNase treatment with a Turbo DNA-free kit (Invitrogen, AM1907). Approximately
494 15 µg of RNA was incubated with 2 µL of DNase and 2 µL of buffer at 37°C for 15 min,
495 followed by a 5-min incubation with the DNase-inactivating agent. The samples were then
496 centrifuged at 8,000 rpm for 3 min, and the supernatant was collected in a fresh microcentrifuge
497 tube. cDNA was prepared with 2 µg of the treated RNA in 20 µL total volume of reaction mix
498 using a high-capacity cDNA reverse transcription kit from Applied Biosystems (4368814). The
499 cDNA was further diluted 1:10 to obtain a final concentration of 10 ng/µL. Gene expression

500 levels were measured using 10 ng of cDNA, 0.5 μM gene specific primers, and 1× SYBR green
501 master mix (Applied Biosystems, A25742). The *gyrA* gene was used as an internal control.
502
503 **Acknowledgements:** This work was supported by National Institutes of Health grants R35
504 GM122461 (J.D.H.), GM034496 (C.O.R.), Cancer Center Support Grant CA21765, and ALSAC,
505 St. Jude Children's Research Hospital. The authors thank Dr. David Rudner for providing MX-
506 2401 and Karen Miller for the preparation of samples for the lipidomic experiments. The content
507 is solely the responsibility of the authors and does not necessarily represent the official views of
508 the National Institutes of Health.

References

1. Zhao H, Patel V, Helmann JD, Dörr T. 2017. Don't let sleeping dogmas lie: new views of peptidoglycan synthesis and its regulation. Mol Microbiol 106:847-860.
2. Schneider T, Sahl HG. 2010. An oldie but a goodie - cell wall biosynthesis as antibiotic target pathway. Int J Med Microbiol 300:161-9.
3. Mitchell AM, Silhavy TJ. 2019. Envelope stress responses: balancing damage repair and toxicity. Nature Reviews Microbiology 17:417-428.
4. Radeck J, Fritz G, Mascher T. 2017. The cell envelope stress response of *Bacillus subtilis*: from static signaling devices to dynamic regulatory network. Curr Genet 63:79-90.
5. Willdigg JR, Helmann JD. 2021. Mini Review: Bacterial Membrane Composition and Its Modulation in Response to Stress. Frontiers in Molecular Biosciences 8.
6. Helmann JD. 2016. *Bacillus subtilis* extracytoplasmic function (ECF) sigma factors and defense of the cell envelope. Curr Opin Microbiol 30:122-132.
7. Radeck J, Gebhard S, Orchard PS, Kirchner M, Bauer S, Mascher T, Fritz G. 2016. Anatomy of the bacitracin resistance network in *Bacillus subtilis*. Molecular Microbiology 100:607-620.
8. Dintner S, Heermann R, Fang C, Jung K, Gebhard S. 2014. A sensory complex consisting of an ATP-binding cassette transporter and a two-component regulatory system controls bacitracin resistance in *Bacillus subtilis*. Journal of Biological Chemistry 289:27899-27910.
9. Kobras CM, Piepenbreier H, Emenegger J, Sim A, Fritz G, Gebhard S. 2020. BceAB-Type Antibiotic Resistance Transporters Appear To Act by Target Protection of Cell Wall Synthesis. Antimicrob Agents Chemother 64.

10. Fritz G, Dintner S, Treichel NS, Radeck J, Gerland U, Mascher T, Gebhard S. 2015. A new way of sensing: need-based activation of antibiotic resistance by a flux-sensing mechanism. MBio 6:e00975-15.
11. George NL, Orlando BJ. 2023. Architecture of a complete Bce-type antimicrobial peptide resistance module. Nat Commun 14:3896.
12. Woods EC, McBride SM. 2017. Regulation of antimicrobial resistance by extracytoplasmic function (ECF) sigma factors. Microbes Infect 19:238-248.
13. Asai K. 2017. Anti-sigma factor-mediated cell surface stress responses in *Bacillus subtilis*. Genes & genetic systems 92:223-234.
14. Campagne S, Allain FH, Vorholt JA. 2015. Extra cytoplasmic function sigma factors, recent structural insights into promoter recognition and regulation. Current Opinion in Structural Biology 30:71-78.
15. Paget MS. 2015. Bacterial sigma factors and anti-sigma factors: structure, function and distribution. Biomolecules 5:1245-1265.
16. Sineva E, Savkina M, Ades SE. 2017. Themes and variations in gene regulation by extracytoplasmic function (ECF) sigma factors. Current opinion in microbiology 36:128-137.
17. Cao M, Wang T, Ye R, Helmann JD. 2002. Antibiotics that inhibit cell wall biosynthesis induce expression of the *Bacillus subtilis* sigma(W) and sigma(M) regulons. Mol Microbiol 45:1267-76.
18. Eiamphungporn W, Helmann JD. 2008. The *Bacillus subtilis* sigma(M) regulon and its contribution to cell envelope stress responses. Mol Microbiol 67:830-48.
19. Luo Y, Asai K, Sadaie Y, Helmann JD. 2010. Transcriptomic and phenotypic

characterization of a *Bacillus subtilis* strain without extracytoplasmic function σ factors. J Bacteriol 192:5736-45.

20. Mascher T, Hachmann AB, Helmann JD. 2007. Regulatory overlap and functional redundancy among *Bacillus subtilis* extracytoplasmic function sigma factors. J Bacteriol 189:6919-27.

21. Luo Y, Helmann JD. 2012. Analysis of the role of Bacillus subtilis σ^M in β-lactam resistance reveals an essential role for c-di-AMP in peptidoglycan homeostasis. Molecular microbiology 83:623-639.

22. Roney IJ, Rudner DZ. 2023. Two broadly conserved families of polyprenyl-phosphate transporters. Nature 613:729-734.

23. Tamehiro N, Okamoto-Hosoya Y, Okamoto S, Ubukata M, Hamada M, Naganawa H, Ochi K. 2002. Bacilysocin, a novel phospholipid antibiotic produced by *Bacillus subtilis* 168. Antimicrob Agents Chemother 46:315-20.

24. Sato T. 2013. Unique Biosynthesis of Sesquarterpenes (C_{35} Terpenes). Bioscience, Biotechnology, and Biochemistry 77:1155-1159.

25. Sato T, Yoshida S, Hoshino H, Tanno M, Nakajima M, Hoshino T. 2011. Sesquarterpenes (C_{35} Terpenes) Biosynthesized via the Cyclization of a Linear C_{35} Isoprenoid by a Tetraprenyl-β-curcumene Synthase and a Tetraprenyl-β-curcumene Cyclase: Identification of a New Terpene Cyclase. Journal of the American Chemical Society 133:9734-9737.

26. Belin BJ, Busset N, Giraud E, Molinaro A, Silipo A, Newman DK. 2018. Hopanoid lipids: from membranes to plant-bacteria interactions. Nat Rev Microbiol 16:304-315.

27. Bosak T, Losick RM, Pearson A. 2008. A polycyclic terpenoid that alleviates oxidative stress. Proc Natl Acad Sci U S A 105:6725-9.

578 28. Kingston AW, Zhao H, Cook GM, Helmann JD. 2014. Accumulation of heptaprenyl
579 diphosphate sensitizes *Bacillus subtilis* to bacitracin: implications for the mechanism of
580 resistance mediated by the BceAB transporter. Mol Microbiol 93:37-49.
581 29. Economou NJ, Cocklin S, Loll PJ. 2013. High-resolution crystal structure reveals
582 molecular details of target recognition by bacitracin. Proc Natl Acad Sci U S A 110:14207-
583 12.
584 30. Piepenbreier H, Diehl A, Fritz G. 2019. Minimal exposure of lipid II cycle intermediates
585 triggers cell wall antibiotic resistance. Nature Communications 10:2733.
586 31. Lands WE. 1965. Lipid metabolism. Annual review of biochemistry 34:313-346.
587 32. Bleffert F, Granzin J, Caliskan M, Schott-Verdugo SN, Siebers M, Thiele B, Rahme L,
588 Felgner S, Dörmann P, Gohlke H, Batra-Safferling R, Jaeger K-E, Kovacic F. 2022.
589 Structural, mechanistic, and physiological insights into phospholipase A-mediated
590 membrane phospholipid degradation in Pseudomonas aeruginosa. eLife 11:e72824.
591 33. Arouri A, Mouritsen OG. 2013. Membrane-perturbing effect of fatty acids and lysolipids.
592 Progress in Lipid Research 52:130-140.
593 34. Henriksen JR, Andresen TL, Feldborg LN, Duelund L, Ipsen JH. 2010. Understanding
594 detergent effects on lipid membranes: a model study of lysolipids. Biophys J 98:2199-205.
595 35. Zheng L, Lin Y, Lu S, Zhang J, Bogdanov M. 2017. Biogenesis, transport and remodeling
596 of lysophospholipids in Gram-negative bacteria. Biochim Biophys Acta Mol Cell Biol
597 Lipids 1862:1404-1413.
598 36. Mykytczuk NCS, Trevors JT, Leduc LG, Ferroni GD. 2007. Fluorescence polarization in
599 studies of bacterial cytoplasmic membrane fluidity under environmental stress. Progress in
600 Biophysics and Molecular Biology 95:60-82.

601 37. Beranová J, Mansilla MC, de Mendoza D, Elhottová D, Konopásek I. 2010. Differences in
602 cold adaptation of *Bacillus subtilis* under anaerobic and aerobic conditions. J Bacteriol
603 192:4164-71.
604 38. Kingston AW, Subramanian C, Rock CO, Helmann JD. 2011. A σ^W-dependent stress
605 response in *Bacillus subtilis* that reduces membrane fluidity. Mol Microbiol 81:69-79.
606 39. Gohrbandt M, Lipski A, Grimshaw JW, Buttress JA, Baig Z, Herkenhoff B, Walter S,
607 Kurre R, Deckers-Hebestreit G, Strahl H. 2022. Low membrane fluidity triggers lipid phase
608 separation and protein segregation in living bacteria. The EMBO Journal 41:e109800.
609 40. Budin I, de Rond T, Chen Y, Chan LJG, Petzold CJ, Keasling JD. 2018. Viscous control of
610 cellular respiration by membrane lipid composition. Science 362:1186-1189.
611 41. Burkholder WF, Kurtser I, Grossman AD. 2001. Replication initiation proteins regulate a
612 developmental checkpoint in *Bacillus subtilis*. Cell 104:269-79.
613 42. Pluckthun A, Dennis EA. 1982. Acyl and phosphoryl migration in lysophospholipids:
614 importance in phospholipid synthesis and phospholipase specificity. Biochemistry 21:1743-
615 50.
616 43. Kielbowicz G, Smuga D, Gladkowski W, Chojnacka A, Wawrzenczyk C. 2012. An LC
617 method for the analysis of phosphatidylcholine hydrolysis products and its application to
618 the monitoring of the acyl migration process. Talanta 94:22-9.
619 44. Sugasini D, Subbaiah PV. 2017. Rate of acyl migration in lysophosphatidylcholine (LPC)
620 is dependent upon the nature of the acyl group. Greater stability of sn-2 docosahexaenoyl
621 LPC compared to the more saturated LPC species. PLoS One 12:e0187826.
622 45. Subramanian C, Frank MW, Yun MK, Rock CO. 2023. The Phospholipase A1 Activity of
623 Glycerol Ester Hydrolase (Geh) Is Responsible for Extracellular 2-12(S)-

Methyltetradecanoyl-Lysophosphatidylglycerol Production in *Staphylococcus aureus*. mSphere 8:e0003123.

46. Jumper J, Evans R, Pritzel A, Green T, Figurnov M, Ronneberger O, Tunyasuvunakool K, Bates R, Žídek A, Potapenko A, Bridgland A, Meyer C, Kohl SAA, Ballard AJ, Cowie A, Romera-Paredes B, Nikolov S, Jain R, Adler J, Back T, Petersen S, Reiman D, Clancy E, Zielinski M, Steinegger M, Pacholska M, Berghammer T, Bodenstein S, Silver D, Vinyals O, Senior AW, Kavukcuoglu K, Kohli P, Hassabis D. 2021. Highly accurate protein structure prediction with AlphaFold. Nature 596:583-589.

47. van Kempen M, Kim SS, Tumescheit C, Mirdita M, Lee J, Gilchrist CLM, Söding J, Steinegger M. 2023. Fast and accurate protein structure search with Foldseek. Nature Biotechnology doi:10.1038/s41587-023-01773-0.

48. Varadi M, Bertoni D, Magana P, Paramval U, Pidruchna I, Radhakrishnan M, Tsenkov M, Nair S, Mirdita M, Yeo J, Kovalevskiy O, Tunyasuvunakool K, Laydon A, Žídek A, Tomlinson H, Hariharan D, Abrahamson J, Green T, Jumper J, Birney E, Steinegger M, Hassabis D, Velankar S. 2023. AlphaFold Protein Structure Database in 2024: providing structure coverage for over 214 million protein sequences. Nucleic Acids Res doi:10.1093/nar/gkad1011.

49. Aschauer P, Zimmermann R, Breinbauer R, Pavkov-Keller T, Oberer M. 2018. The crystal structure of monoacylglycerol lipase from *M. tuberculosis* reveals the basis for specific inhibition. Sci Rep 8:8948.

50. Côtes K, Dhouib R, Douchet I, Chahinian H, de Caro A, Carrière F, Canaan S. 2007. Characterization of an exported monoglyceride lipase from *Mycobacterium tuberculosis* possibly involved in the metabolism of host cell membrane lipids. Biochem J 408:417-27.

647 51. Bauer TL, Buchholz PCF, Pleiss J. 2020. The modular structure of α/β-hydrolases. The
648 FEBS Journal 287:1035-1053.
649 52. Hutter B, Schaab C, Albrecht S, Borgmann M, Brunner NA, Freiberg C, Ziegelbauer K,
650 Rock CO, Ivanov I, Loferer H. 2004. Prediction of mechanisms of action of antibacterial
651 compounds by gene expression profiling. Antimicrob Agents Chemother 48:2838-44.
652 53. Zhang Q, Cornilleau C, Müller RR, Meier D, Flores P, Guérin C, Wolf D, Fromion V,
653 Carballido-Lopez R, Mascher T. 2023. Comprehensive and Comparative Transcriptional
654 Profiling of the Cell Wall Stress Response in *Bacillus subtilis*. bioRxiv
655 doi:10.1101/2023.02.03.526509:2023.02.03.526509.
656 54. Zhao H, Sun Y, Peters JM, Gross CA, Garner EC, Helmann JD. 2016. Depletion of
657 Undecaprenyl Pyrophosphate Phosphatases Disrupts Cell Envelope Biogenesis in *Bacillus*
658 *subtilis.* J Bacteriol 198:2925-2935.
659 55. Radeck J, Lautenschläger N, Mascher T. 2017. The Essential UPP Phosphatase Pair BcrC
660 and UppP Connects Cell Wall Homeostasis during Growth and Sporulation with Cell
661 Envelope Stress Response in *Bacillus subtilis*. Front Microbiol 8:2403.
662 56. Sit B, Srisuknimit V, Bueno E, Zingl FG, Hullahalli K, Cava F, Waldor MK. 2023.
663 Undecaprenyl phosphate translocases confer conditional microbial fitness. Nature 613:721-
664 728.
665 57. Rubinchik E, Schneider T, Elliott M, Scott WR, Pan J, Anklin C, Yang H, Dugourd D,
666 Müller A, Gries K, Straus SK, Sahl HG, Hancock RE. 2011. Mechanism of action and
667 limited cross-resistance of new lipopeptide MX-2401. Antimicrob Agents Chemother
668 55:2743-54.
669 58. Zhao H, Roistacher DM, Helmann JD. 2019. Deciphering the essentiality and function of

the anti-σ^M factors in *Bacillus subtilis*. Mol Microbiol 112:482-497.

59. Zhao H, Sachla AJ, Helmann JD. 2019. Mutations of the *Bacillus subtilis* YidC1 (SpoIIIJ) insertase alleviate stress associated with σ^M-dependent membrane protein overproduction. PLoS Genet 15:e1008263.

60. Cao M, Helmann JD. 2002. Regulation of the *Bacillus subtilis bcrC* bacitracin resistance gene by two extracytoplasmic function σ factors. Journal of Bacteriology 184:6123-6129.

61. Meeske AJ, Riley EP, Robins WP, Uehara T, Mekalanos JJ, Kahne D, Walker S, Kruse AC, Bernhardt TG, Rudner DZ. 2016. SEDS proteins are a widespread family of bacterial cell wall polymerases. Nature 537:634-638.

62. Meeske AJ, Sham LT, Kimsey H, Koo BM, Gross CA, Bernhardt TG, Rudner DZ. 2015. MurJ and a novel lipid II flippase are required for cell wall biogenesis in *Bacillus subtilis*. Proc Natl Acad Sci U S A 112:6437-42.

63. Emami K, Guyet A, Kawai Y, Devi J, Wu LJ, Allenby N, Daniel RA, Errington J. 2017. RodA as the missing glycosyltransferase in *Bacillus subtilis* and antibiotic discovery for the peptidoglycan polymerase pathway. Nat Microbiol 2:16253.

64. Piepenbreier H, Sim A, Kobras CM, Radeck J, Mascher T, Gebhard S, Fritz G. 2020. From Modules to Networks: a Systems-Level Analysis of the Bacitracin Stress Response in *Bacillus subtilis*. mSystems 5.

65. Bernard R, El Ghachi M, Mengin-Lecreulx D, Chippaux M, Denizot F. 2005. BcrC from *Bacillus subtilis* acts as an undecaprenyl pyrophosphate phosphatase in bacitracin resistance. J Biol Chem 280:28852-7.

66. Schirner K, Marles-Wright J, Lewis RJ, Errington J. 2009. Distinct and essential morphogenic functions for wall- and lipo-teichoic acids in *Bacillus subtilis*. Embo j 28:830-

693 42.

694 67. Li FKK, Rosell FI, Gale RT, Simorre JP, Brown ED, Strynadka NCJ. 2020.
695 Crystallographic analysis of *Staphylococcus aureus* LcpA, the primary wall teichoic acid
696 ligase. J Biol Chem 295:2629-2639.

697 68. Fung DK, Yang J, Stevenson DM, Amador-Noguez D, Wang JD. 2020. Small Alarmone
698 Synthetase SasA Expression Leads to Concomitant Accumulation of pGpp, ppApp, and
699 AppppA in *Bacillus subtilis*. Frontiers in Microbiology 11.

700 69. Rojas-Tapias DF, Helmann JD. 2019. Roles and regulation of Spx family transcription
701 factors in *Bacillus subtilis* and related species. Advances in microbial physiology 75:279-
702 323.

703 70. Zhu J, Wang S, Wang C, Wang Z, Luo G, Li J, Zhan Y, Cai D, Chen S. 2023. Microbial
704 synthesis of bacitracin: Recent progress, challenges, and prospects. Synth Syst Biotechnol
705 8:314-322.

706 71. Koo BM, Kritikos G, Farelli JD, Todor H, Tong K, Kimsey H, Wapinski I, Galardini M,
707 Cabal A, Peters JM, Hachmann AB, Rudner DZ, Allen KN, Typas A, Gross CA. 2017.
708 Construction and Analysis of Two Genome-Scale Deletion Libraries for *Bacillus subtilis*.
709 Cell Syst 4:291-305.e7.

710 72. Quisel JD, Burkholder WF, Grossman AD. 2001. In vivo effects of sporulation kinases on
711 mutant Spo0A proteins in *Bacillus subtilis*. J Bacteriol 183:6573-8.

712 73. Tiwari KB, Sen S, Gatto C, Wilkinson BJ. 2021. Fluorescence Polarization (FP) Assay for
713 Measuring *Staphylococcus aureus* Membrane Fluidity. Methods Mol Biol 2341:55-68.

714 74. Kuhry JG, Duportail G, Bronner C, Laustriat G. 1985. Plasma membrane fluidity
715 measurements on whole living cells by fluorescence anisotropy of

716 trimethylammoniumdiphenylhexatriene. Biochim Biophys Acta 845:60-7.

717 75. Radeck J, Kraft K, Bartels J, Cikovic T, Durr F, Emenegger J, Kelterborn S, Sauer C, Fritz
718 G, Gebhard S, Mascher T. 2013. The Bacillus BioBrick Box: generation and evaluation of
719 essential genetic building blocks for standardized work with *Bacillus subtilis*. J Biol Eng
720 7:29.

721

722

723

724

Table 1. Strains used in this study

Strain Number	Genotype	Construction	Reference
168	*trpC2*	Lab strain	Lab stock
HB27141	*trpC2 ytpA::erm*	BGSC → 168	Lab stock
HB27232	*trpC2 ytpA null*	pDR244 → HB27141	This study
HB27450	*trpC2 amyE::pSpac(hy)-ytpA*	pPL82-*ytpA* → 168	This study
HB27142	*trpC2 des::kan*	BGSC → 168	This study
HB27373	*trpC2 des::kan bkd::erm (Δbkd)*	gDNA *bkd::erm* (see primers) → HB27142	This study
HB27384	*trpC2 des::kan bkd::erm amyE:: pSpac(hy)-ytpA*	pPL82-*ytpA* → HB27373	This study
HB27482	*trpC2 ytpA null des::kan bkd::erm*	gDNA *bkd::erm* (see primers) → HB27232	This study
HB27246	*trpC2 sacA::PytpAB-luxABCDE-erm*	pBS3E-lux-*PytpAB* → 168	This study
HB27247	*trpC2 sacA::PytpAB reduced-luxABCDE-erm*	pBS3E-lux-*PytpAB* reduced → 168	This study
HB27260	*trpC2 sigM::erm*	BGSC → 168	Lab stock
HB27287	*trpC2 sigM::erm sacA::PytpAB-luxABCDE-erm*	pBS3K-lux-*PytpAB* → HB27260	This study
HB27272	*trpC2 bcrC::erm*	BGSC → 168	Lab stock
HB27277	*trpC2 bcrC null*	pDR244 → HB27272	This study
HB27291	*trpC2 bcrC null sacA::PytpAB-luxABCDE-erm*	pBS3K-lux-*PytpAB* → HB27277	This study
HB27271	*trpC2 bceAB::kan*	HB0928	Lab stock
HB27289	*trpC2 bceAB::kan sacA::PytpAB-luxABCDE*	pBS3E-lux-*PytpAB* → HB27271	This study
HB27249	*trpC2 ytpB::erm*	BGSC → 168	Lab stock
HB27253	*trpC2 ytpB null*	pDR244 → HB27249	This study
HB27407	*trpC2 ytpAB::erm*	See primers	This study
HB27275	*trpC2 ytpA null bcrC::erm*	gDNA HB27272 → HB27232	This study
HB27360	*trpC2 ytpA null bcrC null*	pDR244 → HB27275	This study
HB27442	*trpC2 uppP::erm*	BGSC → 168	Lab stock
HB27446	*trpC2 uppP null*	pDR244 → HB27442	This study
HB27443	*trpC2 ytpA null uppP::erm*	gDNA HB27442 → HB27232	This study
HB27447	*trpC2 ytpA null uppP null*	pDR244 → HB27443	This study
HB27344	*trpC2 uptA::erm*	BGSC → 168	Lab stock
HB27393	*trpC2 uptA null*	pDR244 → HB27344	This study
HB27351	*trpC2 ytpA null uptA::erm*	gDNA HB27344 → HB27232	This study
HB27362	*trpC2 ytpA null uptA null*	pDR244 → HB27351	This study
HB27273	*trpC2 ytpA null bceAB::kan*	gDNA HB27271 → HB27232	This study
HB27490	*trpC2 ytpA uptA bceAB::kan*	gDNA HB27271 → HB27362	This study

725

726

Figure legends

Figure 1. Induction of *ytpA* increases membrane fluidity. Overexpression of *ytpA* using the *spac(Hy)* promoter (HB27450) with 1 mM IPTG yields statistically significant differences in anisotropy compared to the WT and *ytpA* knockout (Δ*ytpA,* HB27232) strains. N = 3 biological replicates. A one-way ANOVA with a Tukey test for multiple comparisons was performed. Columns labeled with different letters are statistically distinct from each other; with a *P* value cutoff < 0.05.

Figure 2. YtpA is physiologically important in cells with defects in membrane fluidity (A). A clean, unmarked deletion of *ytpA (*Δ*ytpA)* in the Δ*bkd* strain (HB27482), reduces the growth of the cells at the permissive temperatures of 27°C, 37 °C and 45 °C on LB medium. The colony size of the Δ*bkd* Δ*ytpA* strain is significantly smaller than the Δ*bkd* strain (HB27373). (B) Overexpression of *ytpA* in Δ*bkd* cells (HB27384) restores viability on minimal media when grown at non-permissive low temperature (22 °C). A representative image is shown (N = 3). Untreated column represents cells plated on minimal media without any supplementation. IPTG column represents cells plated on minimal media supplemented with 1 mM IPTG and MB column represents cells plated on minimal media supplemented with 100 μM 2-methylbutyric acid. (C) Induction of *ytpA* from the IPTG-inducible *spac(Hy)* promoter partially restores fluidity in a *Δbkd* strain. The data presented is the average of three biological replicates where errors bars represent the standard deviation. A one-way ANOVA with a Tukey test for multiple comparisons was performed. Columns labeled with different letters are statistically distinct from each other with a *P* value cutoff of < 0.05.

Figure 3. Lysophospholipid content of cells and media in WT and Δ*ytpA* strain (HB27232). Strains were grown in LB to late-log phase, the cells or media were extracted with methanol and the LPG/LPE molecular species determined by LC-MS/MS. The LPG/LPE abundances were determined relative to a [d5]17-LPG internal standard. WT (red); Δ*ytpA* (blue). (A) cellular LPG, (B) media LPG, (C) cellular LPE, (D) media LPE. Student t-test was done to compare the values of WT and *ytpA* samples for each molecular species separately. * indicates *P* value < 0.05.

Figure 4. Induction of the *ytpAB* operon is σ^M dependent. Induction of *PytpAB-lux* (HB27246) is lost following bacitracin treatment in the absence of *sigM* (HB27287) and the σ^M-specific consensus sequence at the *ytpAB* promoter (HB27247). N = 3 biological replicates; error bars represent standard deviation.

Figure 5. Effects of Δ*ytpA* and Δ*ytpB* (unmarked, in-frame deletions) on bacitracin sensitivity. Individual deletions of *ytpA* (HB27232) or *ytpB* (HB27253) do not have a significant effect on bacitracin (BAC) sensitivity compared to the WT cells. The *ytpAB* operon deletion (HB27407) has an increased lag in the presence of 62.5 μg/mL bacitracin compared to either single mutant. N =6; standard deviation in the growth of each strain has been shown by shading.

Figure 6. Loss of YtpA increases bacitracin (BAC) sensitivity in genetically sensitized strains. (A) Deletion of *ytpA* (HB27360) increases the sensitivity of the bacitracin-sensitive *bcrC* mutant (HB27277) as measured with 5 μg/ml bacitracin (B) Neither the loss of *ytpA* (HB27232) or *uppP* (HB27446) alone, nor the combination (HB27447), has a major impact on bacitracin sensitivity

as measured with 62.5 μg/ml bacitracin. (C) Deletion of *ytpA* (HB27273) increases the sensitivity of the bacitracin-sensitive *bceAB* mutant (HB27271) as measured with 5 μg/ml bacitracin. N = 5 biological replicates; standard deviation in the growth of each strain has been shown by shading.

Figure 7. Epistasis of *ytpA* and *uptA* as measured by the growth of the *ytpA* (HB27232), *uptA* (HB27393) mutants alone and in combination (HB27362) on treatment with (A) 0.6 μg/ml MX-2401 and (B) 62.5 μg/ml bacitracin. N = 5 biological replicates; standard deviation in the growth of each strain has been shown by shading.

Figure 8. Model for lipid II recycling. Lipid-II consists of the peptidoglycan precursors bound to undecaprenyl pyrophosphate (UPP) moiety and is synthesized in the inner leaflet of the membrane. Flippases MurJ/Amj flip it to the outer leaflet where PBPs incorporate the precursors into the peptidoglycan meshwork. Subsequently, UPP is dephosphorylated to UP, and UptA (or other unidentified proteins) flips UP back to the inner membrane, where MraY initiates the incorporation of peptidoglycan precursors. Bacitracin binds to UPP in the outer membrane, inhibiting its recycling and limiting cell wall synthesis. In response to bacitracin treatment, BceAB is upregulated to remove bacitracin from UPP, and BcrC is upregulated to dephosphorylate UPP into UP, thereby eliminating the bacitracin target. In addition, YtpA, which increases membrane fluidity by an unknown mechanism, may contributes to bacitracin resistance. We speculate that YtpA may aid in flipping of UPP from the outer to the inner leaflet of the membrane.

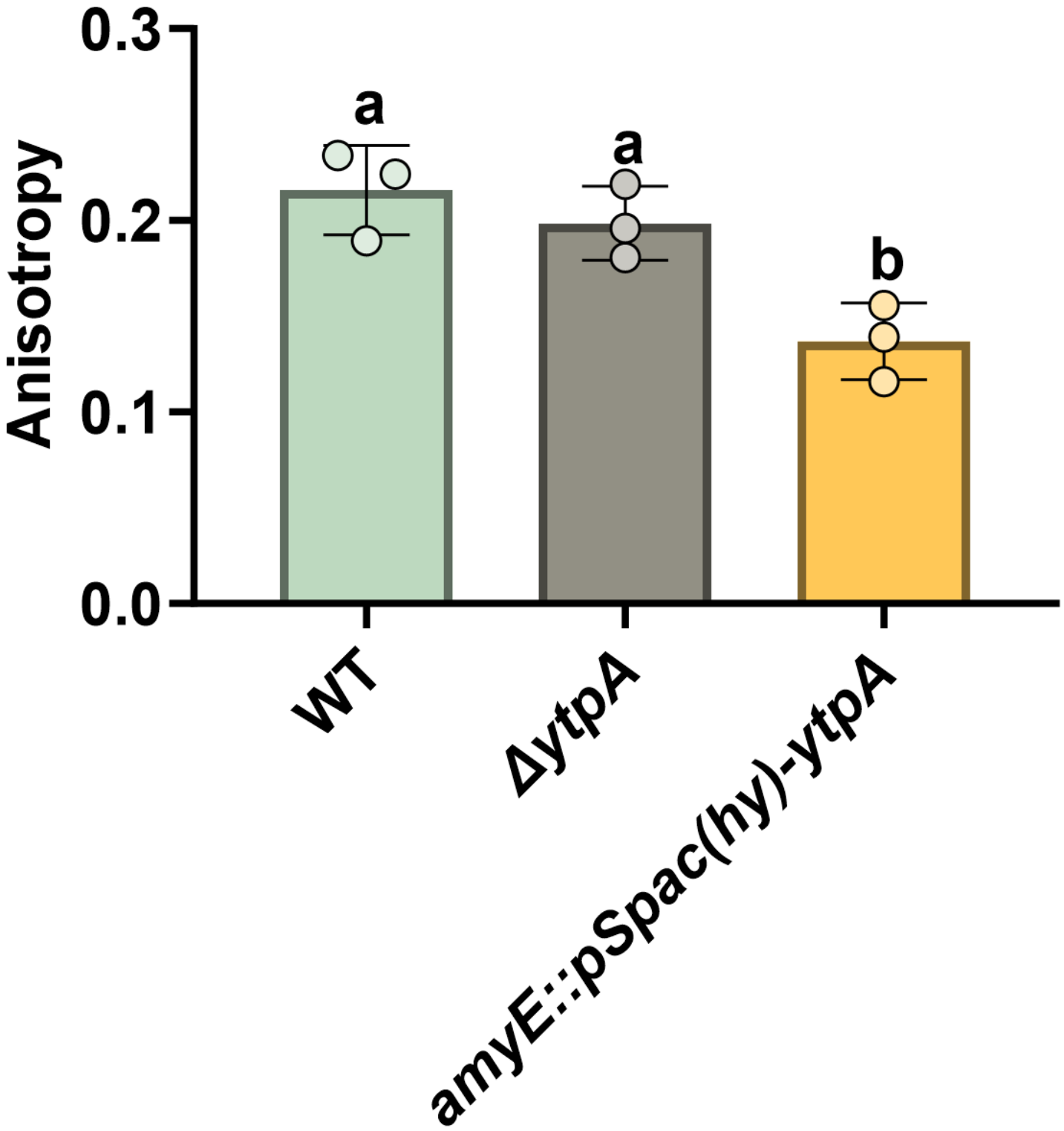

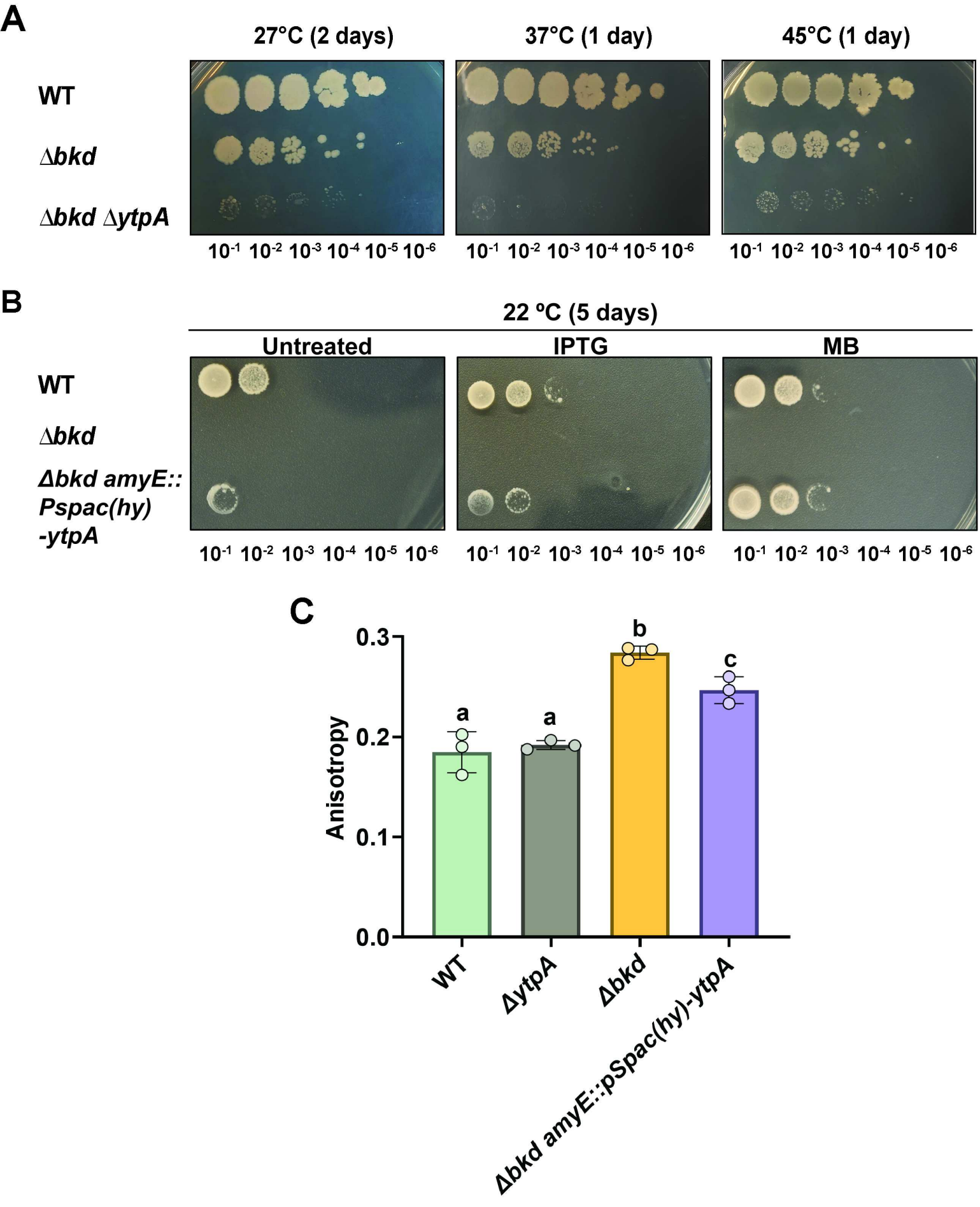

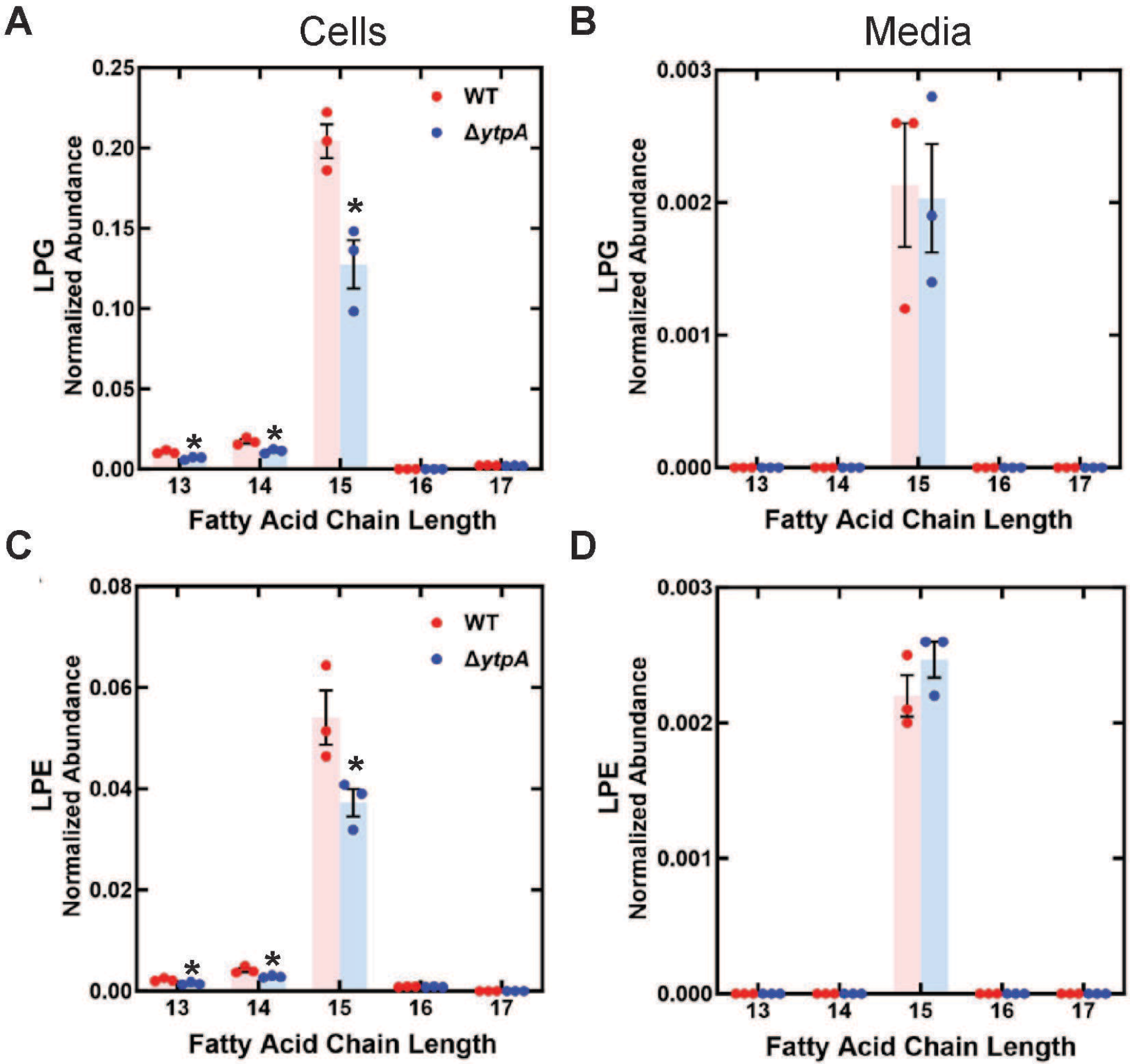
A
Cells
B
Media
C
D
LPG
LPE
Normalized Abundance
WT
ΔytpA
0.25
0.20
0.15
0.10
0.05
0.00
0.003
0.002
0.001
0.000
0.08
0.06
0.04
0.02
13
14
15
16
17
Fatty Acid Chain Length
*

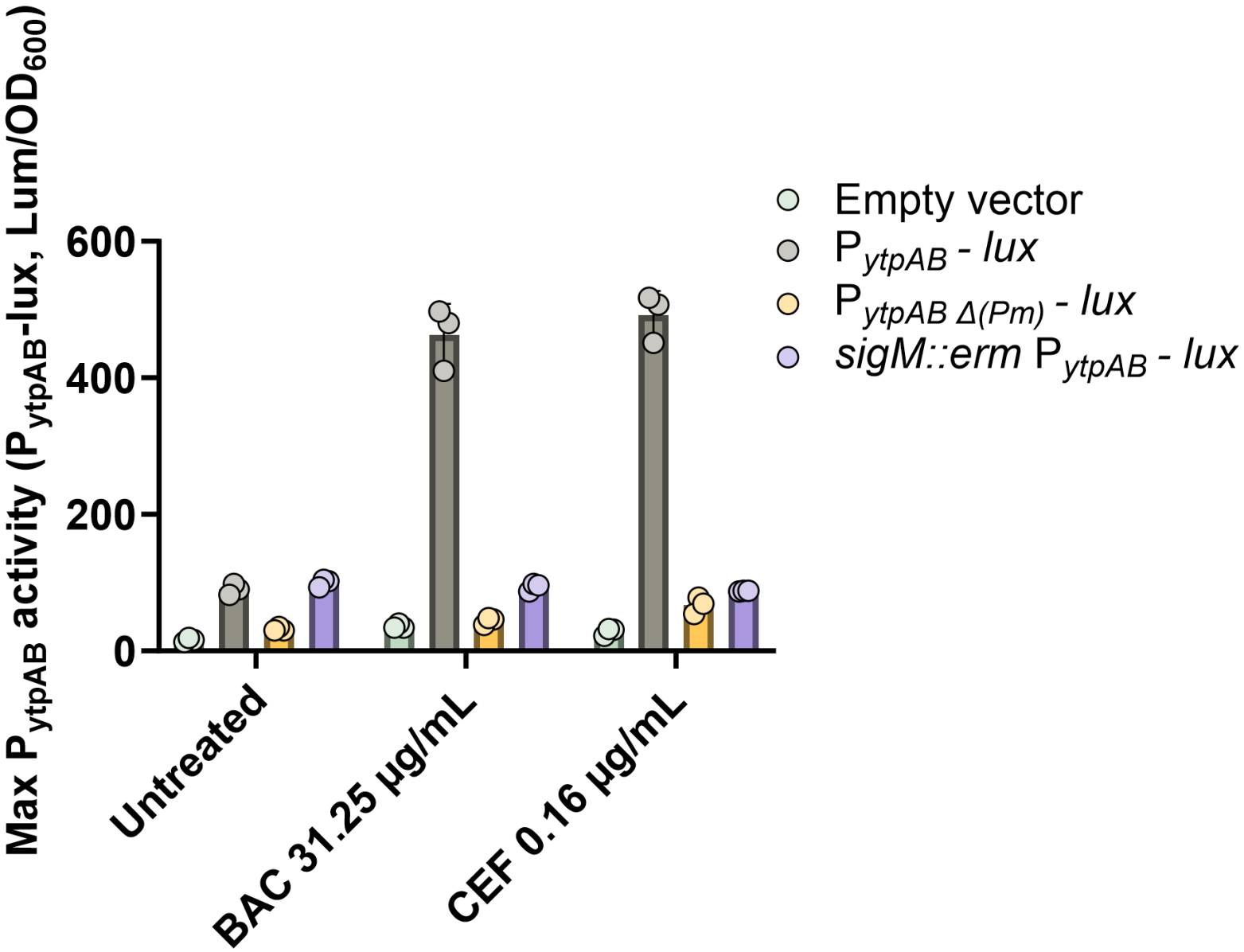

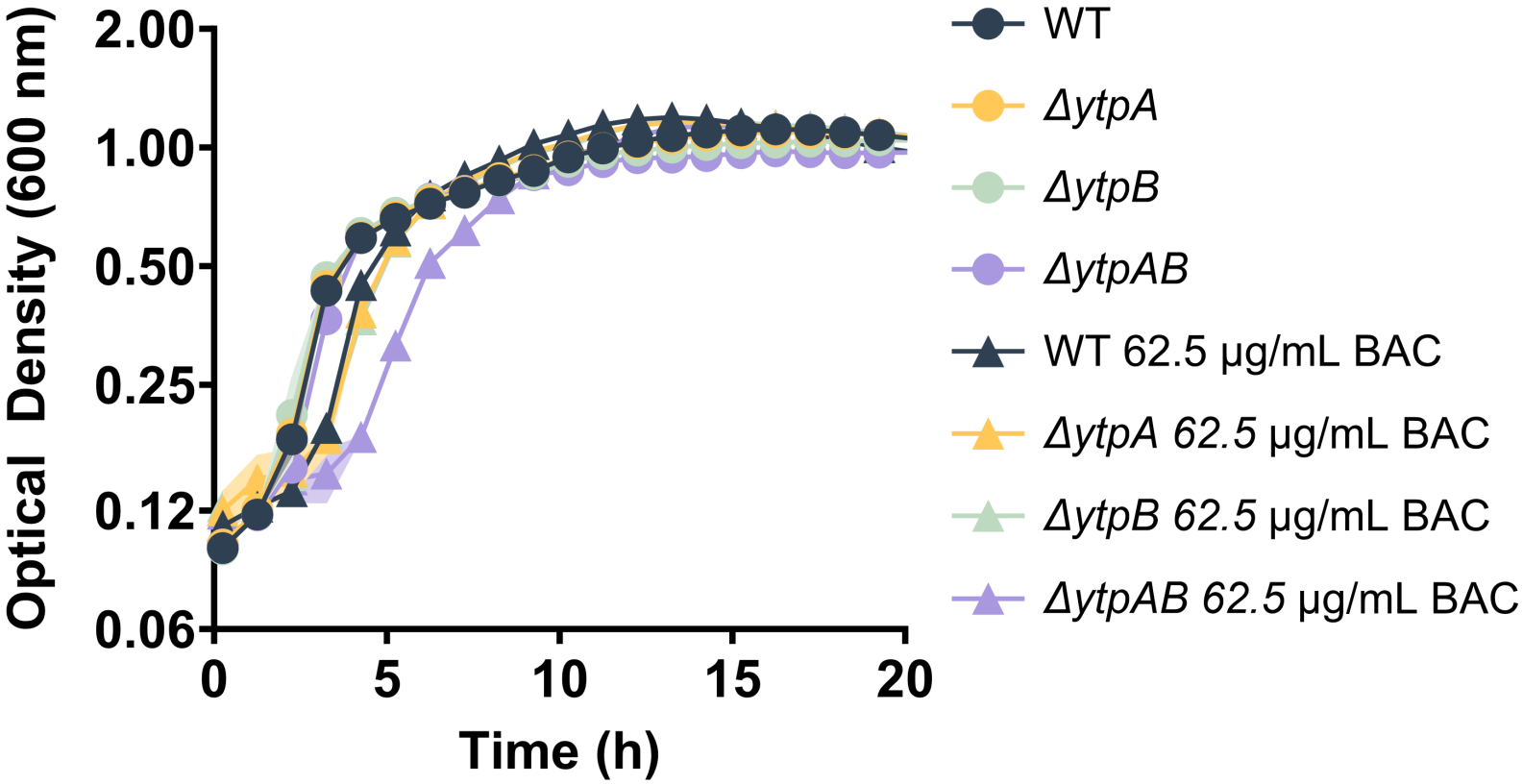

A

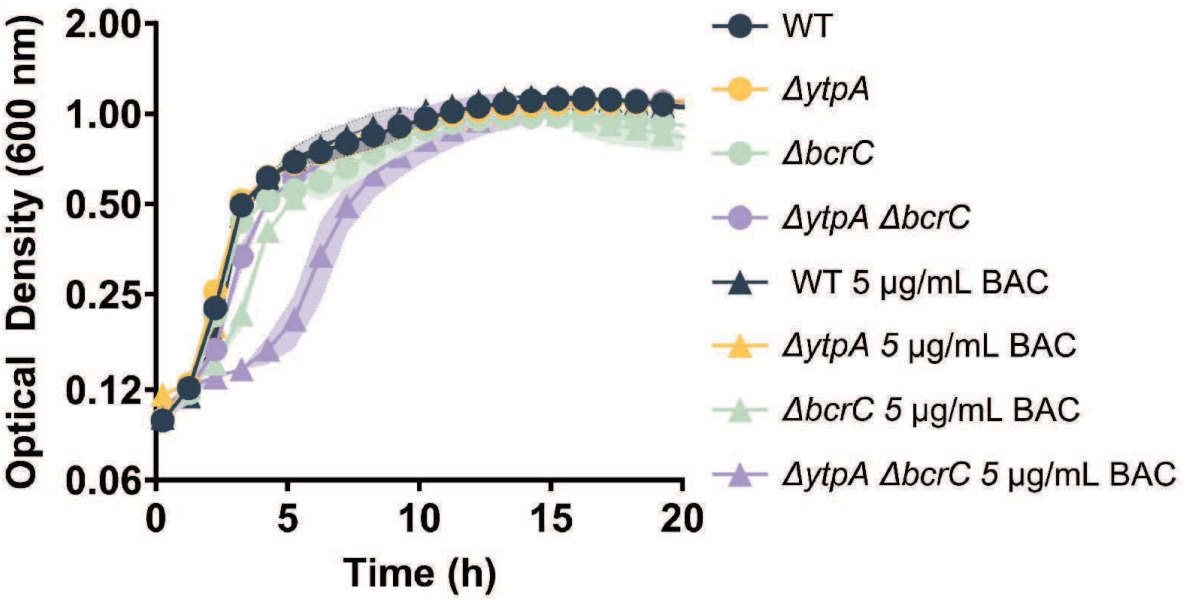

B

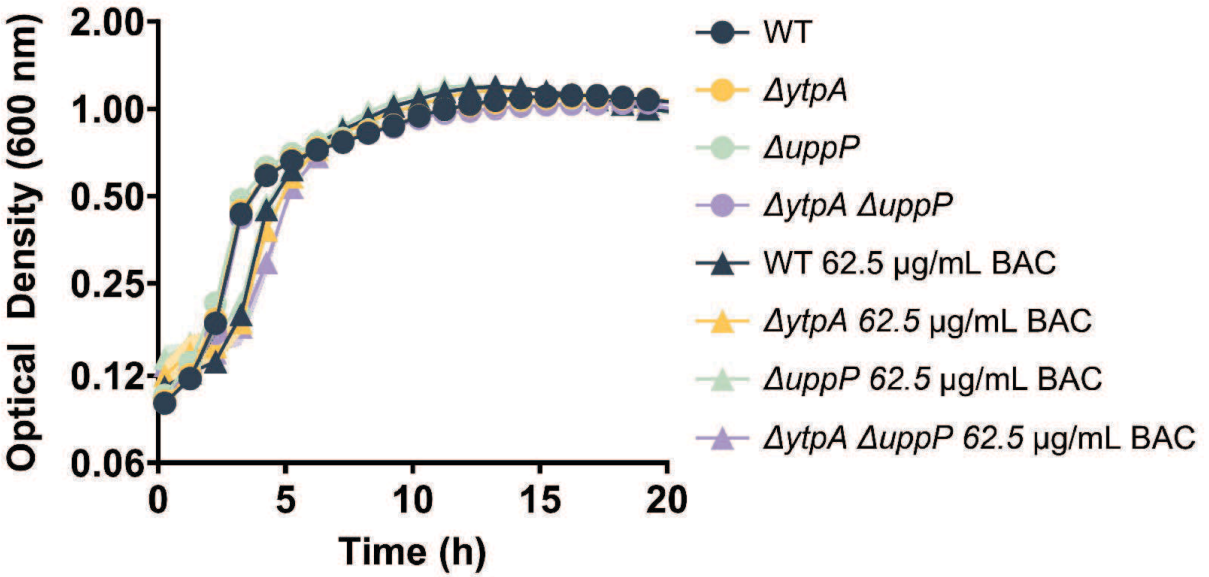

C

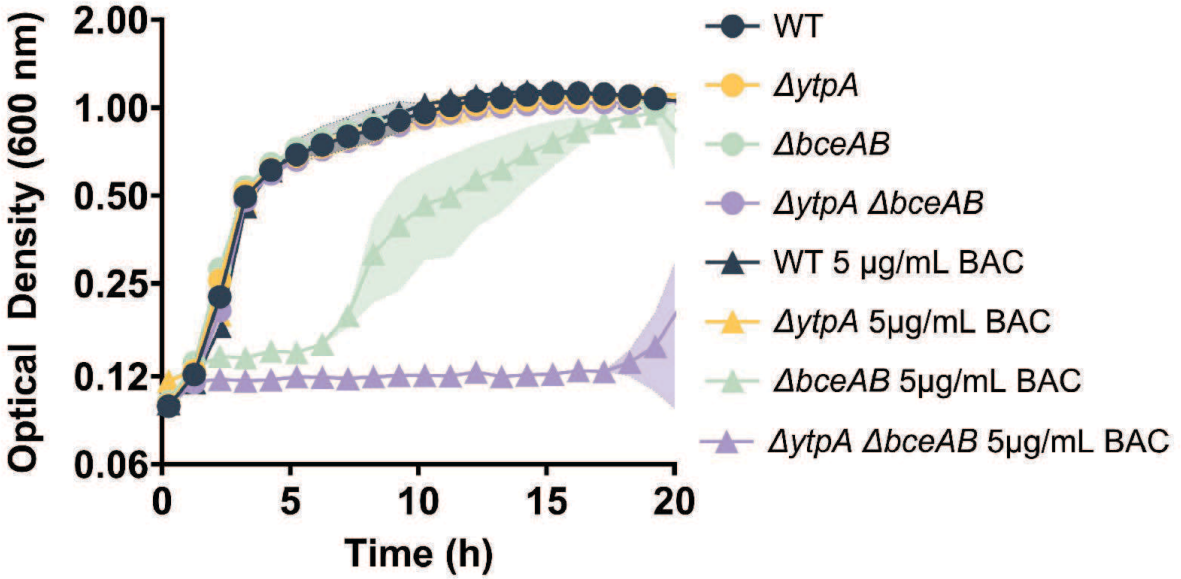

A

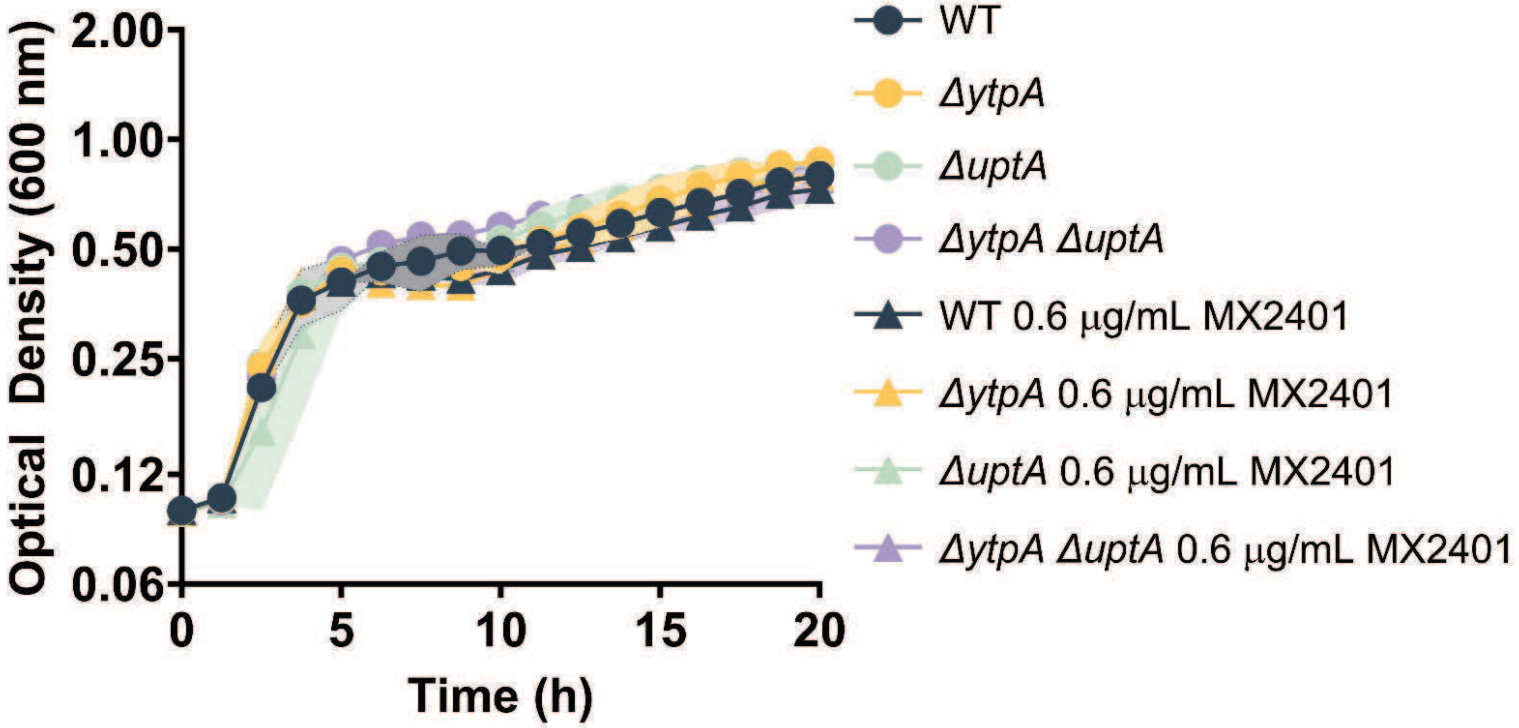
Optical Density (600 nm)
2.00
1.00
0.50
0.25
0.12
0.06
0
5
10
15
20
Time (h)
WT
ΔytpA
ΔuptA
ΔytpA ΔuptA
WT 0.6 μg/mL MX2401
ΔytpA 0.6 μg/mL MX2401
ΔuptA 0.6 μg/mL MX2401
ΔytpA ΔuptA 0.6 μg/mL MX2401

B

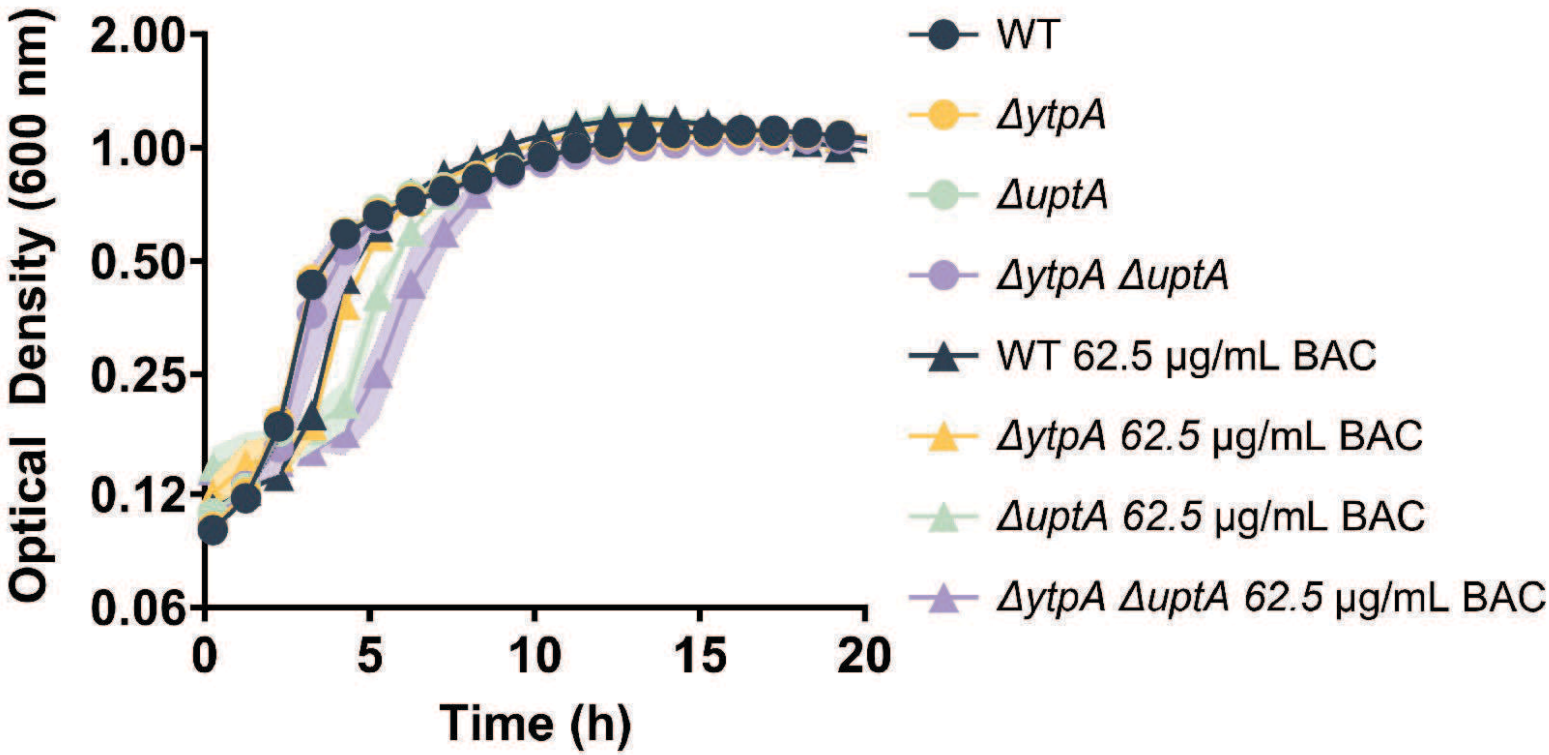
Optical Density (600 nm)
2.00
1.00
0.50
0.25
0.12
0.06
0
5
10
15
20
Time (h)
WT
ΔytpA
ΔuptA
ΔytpA ΔuptA
WT 62.5 μg/mL BAC
ΔytpA 62.5 μg/mL BAC
ΔuptA 62.5 μg/mL BAC
ΔytpA ΔuptA 62.5 μg/mL BAC